A Study on High-Frequency Wave Propagation along Overhead Conductors by Earth-Return Admittance/ Impedance and Numerical Electromagnetic Analysis

A. Ametani, Y. Miyamoto, T. Asada, Y. Baba, N. Nagaoka, I. Lafaia, J. Mahseredjian, K. Tanabe

***Abstract*--Well-known earth-return impedance formulas by Pollaczek, Carson et al. are investigated and it has been made clear that Pollaczek/Carson's formulas can deal with displacement currents when the relative earth permittivity is 1. Wave propagation characteristics at a high frequency on overhead conductors have been evaluated by Wise's earth-return admittance and modified Pollaczek/Carson's (accurate) impedance, i.e. by TL (transmission line) approach. The results are compared with those calculated by numerical electromagnetic analysis approaches, NEC (numerical electromagnetic code) and FDTD (finite-difference time-domain) method. Both approaches show transition of wave propagation between TEM (transverse electromagnetic) and TM (transverse magnetic) modes in the high frequency region. Thus, it becomes clear that the accurate earth-return impedance is applicable to such a high frequency, and that in the frequency region higher than the frequency of the mode transition, the earth-return impedance has no contribution to the wave and surge propagation, because the wave propagation is no more earth-return but a so-called surface wave as predicted by Sommerfeld and Goubau.**

***Keywords*: wave propagation, high frequency, overhead conductor, earth-return admittance/impedance, Sommerfeld-Goubau propagation, numerical electromagnetic analysis.**

I. Introduction

The earth-return impedance is essential to study tele-communication, wave propagation and transients on overhead conductors or underground cables. There are a number of papers deriving the impedance formulas, either accurate or approximate, and discussing the formulas and their application [1- 10]. Among those, Pollaczek's infinite integral formula [1] is referred as the most accurate but it is numerically unstable. Because of this, Carson's infinite series expansion [2] has been widely used. Sunde also derived the earth-return impedance which was the same as Carson's one as Sunde stated in his book [3]. Wise modified Carson's formula for a high frequency [4]. It is often said that Pollaczek's and Carson's earth-return impedance formulas cannot be applied to a high frequency region, because they neglect displacement currents.

It has been understood for long that the attenuation constant of an overhead conductor increases monotonously with frequency. Kikuchi discussed high-frequency wave propagation more than 50 years ago [11, 12], and pointed out that the wave propagation along the conductor shows a transition between TEM and TM/TE modes above a given frequency. This is the so-called "Sommerfeld-Goubau propagation" [13-15]. To analyze the phenomenon, both earth-return admittance and impedance which can deal with the displacement currents are necessary.

In this paper, it is investigated how Carson's and Pollaczek's formulas deal with displacement currents based on a stratified earth impedance [16-18]. Then, by adopting an earth-return admittance [19, 20], high frequency wave propagation is investigated [21, 22] and is simulated by numerical electromagnetic analysis methods [23- 25] for a comparison [26, 27].

II. Earth-Return Impedance/Admittance Formulas

A. Impedance

Fig. 1 illustrates a multi-conductor overhead line above a three-layer stratified earth. In general, the earth-return impedance formula of the overhead line is given in the following form.

$$Z_{ij} = j\omega(\mu_0/2\pi)\left[P_0 + (Q - jR)\right],\ P_0 = \ln\left(D_{ij}/d_{ij}\right) \quad (1)$$

$$Q - jR = 2\int_0^\infty K \cdot F(s) \cdot ds,\ K = 1/(a+s) \quad (2)$$

$$F(s) = \exp\left\{-\left(h_i + h_j\right)s\right\} \cdot \cos(ys) \quad (3)$$

where $d_{ij}^2 = \left(h_i - h_j\right)^2 + y^2$, $D_{ij}^2 = \left(h_i + h_j\right)^2 + y^2$.

In (2), a is a function of earth conductivity $\sigma_e = 1/\rho_e$, permittivity $\varepsilon_e = \varepsilon_r \cdot \varepsilon_0$ and permeability μ_e derived by various authors.

A1. Stratified Earth

Nakagawa *et al* derived a generalized formula of the earth-return impedance of a multi-phase overhead line above a three-layer stratified earth in Fig. 1 in the following form [16, 17].

$$K = K_3 = (c_1 + c_2)/\{(s + \mu_0 b_1)c_1 + (s - \mu_0 b_1)c_2\} \quad (4)$$

$$c_1 = (b_1 + b_2)(b_2 + b_3) + (b_1 - b_2)(b_2 - b_3)\exp\{2a_2(d_1 - d_2)\}$$

$$c_2 = [(b_1 - b_2)(b_2 + b_3) + (b_1 + b_2)(b_2 - b_3)\exp\{2a_2(d_1 - d_2)\}] \cdot \exp(-2a_1 d_1)$$

$$a_k = \sqrt{s^2 + m_k^2 - m_0^2},\ b_k = a_k/\mu_k \quad (k = 1, 2 \text{ and } 3)$$

A. Ametani, I. Lafaia, J. Mahseredjian are with Polytechnique Montreal, 2500, chemin de Polytechnique, Montréal (Québec) H3T1J4, Canada (e-mail: aametani@mail.doshisha.ac.jp).

Y. Miyamoto, T. Asada, Y. Baba, N. Nagaoka are with Doshisha University, Karasuma-higashi-iru, Imadegawa-dori, Kamigyo-ku, Kyoto-shi 602-8580, Japan.

K. Tanabe is with Central Research Institute of Electrical Power Industries, Otemachi Bldg., 1-6-1 Otemachi, Chiyoda-ku, Tokyo 100-8126, Japan.

Paper submitted to the International Conference on Power Systems Transients (IPST2015) in Cavtat, Croatia June 15-18, 2015

$$m_0^2 = j\omega\mu_0(\sigma_0 + j\omega\varepsilon_0), \quad m_k^2 = j\omega\mu_k(\sigma_k + j\omega\varepsilon_k)$$

where μ_k, σ_k, and ε_k are the permeability, conductivity and permittivity of medium k and μ_0, ε_0 are the counterparts for free space (air).

For a two-layer earth,

$$K = K_2 = \frac{b_1 + b_2 + (b_1 - b_2)\exp(-2a_1 d_1)}{(s+\mu_0 b_1)(b_1 + b_2) + (s - \mu_0 b_1)(b_1 - b_2)\exp(-2a_1 d_1)} \quad (5)$$

For a homogeneous earth,

$$K = K_1 = (s + \mu_0 b_1)^{-1} = 1\Big/\left\{s + (\mu_0/\mu_1)\sqrt{s^2 + m_1^2 - m_0^2}\right\} \quad (6)$$

When the earth permeability μ_e is taken to be the same as that of air, and the free space conductivity σ_0 is zero, as assumed in the derivation of all the existing formulas [1-10], then the following equation is given,

$$K = 1/(s + a_1),\ a_1 = \sqrt{s^2 + m_1^2 - m_0^2} \quad (7)$$

where

$$m_1^2 = j\omega\mu_e(\sigma_e + j\omega\varepsilon_e),\ m_0^2 = j\omega\mu_0 \cdot j\omega\varepsilon_0 \quad (8)$$

By substituting (8) into (7), the following result is obtained.

$$a_1 = \sqrt{s^2 + j\omega\mu_0\{\sigma_e + j\omega\varepsilon_0(\varepsilon_r - 1)\}} \quad (9)$$

A2. Pollaczek and Carson

Pollaczek derived the following equation for a [1].

$$a_p = \sqrt{s^2 + j\omega\mu_0\sigma_e} \quad (10)$$

Pollaczek assumes the earth permeability and permittivity are the same as those of a free space. This will be explained later in detail.

As is well-known, Carson's formula in an infinite integral form is the same as Pollaczek's one [2], i.e. $a_c = a_p$.

In Carson's time, there was no computer. Thus Carson derived a formula with infinite series expansion which has been widely used since then, and Carson's formula has meant equivalent to the earth-return impedance.

A3. Sunde

Sunde derived the following formula [3].

$$a_s = \sqrt{s^2 + j\omega\mu_0(\sigma_e + j\omega\varepsilon_e)} \quad (11)$$

A4. Wise's Correction

Wise modified Carson's formula so as to be able to deal with displacement currents for arbitrary $\varepsilon_e = \varepsilon_r\varepsilon_0$ in a high frequency region, and derived the following formula [4].

$$a_w = \sqrt{s^2 + j\omega\mu_0\{\sigma_e + j\omega\varepsilon_0(\varepsilon_r - 1)\}} \quad (12)$$

It should be noted that the above result is identical to that in (9). Also, Kikuchi's formula of the earth-return impedance, which is said to be the most accurate, becomes identical to (9) under the assumption of $\mu_e = \mu_0$ and $\sigma_0 = 0$ [11, 12].

A5. Discussions

It is said quite often that Pollaczek's and Carson's formulas cannot deal with displacement currents and thus the formulas are not applicable to high frequencies. This is true when the relative permittivity of the earth is other than unity, i.e. $\varepsilon_e \neq \varepsilon_0$. For $\varepsilon_e = \varepsilon_0$, "$a$" in (9) or (12) becomes:

$$a = \sqrt{s^2 + j\omega\mu_0\sigma_e} \quad (13)$$

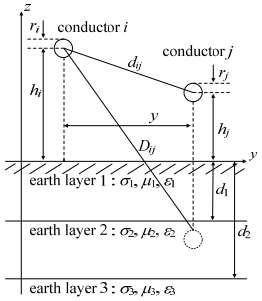

Fig. 1. An overhead multi-conductor system above stratified earth (homogeneous earth: $\sigma_1 = \sigma_2 = \sigma_3 = \sigma_4$, $\varepsilon_1 = \varepsilon_2 = \varepsilon_3 = \varepsilon_4$, $\mu_1 = \mu_2 = \mu_3 = \mu_4$, $d_1 = d_2 = 0$).

This result means that the displacement currents are considered, although it is said that Pollaczek and Carson neglected the displacement currents. The term $j\omega\varepsilon_0$ is cancelled out because of m_0 for the air, as observed in (7). It should be clear now that Pollaczek's and Carson's formulas become (13) if we consider the displacement currents with $\varepsilon_e = \varepsilon_0$. If we neglect the currents, i.e. $\varepsilon_e = 0$, Sunde's formula in (11) becomes (13). As stated in Wise's paper [4], if we consider the displacement currents, the formula should be (7) for $\mu_e = \mu_0$ and $\sigma_0 = 0$, and (6) for arbitrary μ_e and ε_e . Sunde's formula in (11) is not correct, although it is said that Sunde's formula considers the displacement currents and Pollaczek/Carson's formula do not [18]. Also, it should be noted that Sunde said in his book that "formulas and curves for W (= $Q - jR$ in (2) and (11)) have been given by Carson" (p. 112, Section 4.5 in his book [3]). Pollaczek started the impedance formula derivation with the intrinsic propagation constants m_0 for air and m_1 for earth (in (6)). At a certain moment to make the derivation easier, it seems that he assumed $\varepsilon_e = \varepsilon_0$ and used a_p in (10).

In summary, the earth-return impedance formula given by Pollaczek and Carson in (10) can deal with displacement currents for $\varepsilon_e = \varepsilon_0$. Wise's formula in (12) is a generalize formula for arbitrary ε_e, and the formula in (6) is the most general [18]. It is noteworthy that Kikuchi's formula [11, 12] can deal not only with TEM (transverse electromagnetic) mode of propagation but also with TM/TE mode propagation.

B. Admittance

Wise's formula of the earth-return admittance is given in the following form [19] which is the same as that derived by Nakagawa [20].

$$[Y] = j\omega[C],\ [C] = [P]^{-1},\ P_{ij} = (P_0 + M + jN)/2\pi\varepsilon_0 \quad (14)$$

$$M + jN = 2\int_0^\infty (A + jB)\,ds,\ A + jB = F(s)/(a + bs) \quad (15)$$

$$b = m_1^2/m_0^2 = (\sigma_e + j\omega\varepsilon_e)/j\omega\varepsilon_0, \text{ for } \mu_e = \mu_0 \quad (16)$$

$F(s)$ is defined in (3), a in (10), and P_0 in (1).

III. Transition of Propagation Modes

Kikuchi found that the attenuation of an overhead single conductor increases monotonously up to a certain frequency, then it decreases and again increases monotonously [11, 12]. The phenomenon was explained as a transition between a transverse electromagnetic (TEM) mode of propagation and a transverse magnetic (TM) or a transverse electric (TE) mode,

based on the work by Sommerferd [13] and Goubau [14, 15]. Nakagawa made a similar observation [21].

Fig. 2 shows the frequency characteristic of attenuation constant α. In the figure, Δ and $\circ$ are NEC simulation results which are explained in Section IV A2.2. The real line in the figure is the case considering Wise's admittance in (14) with the modified Pollaczek/Carson's (accurate) earth-return impedance in (9), while the dotted line is the case of a conventional admittance given only by P_0 in (14) assuming a perfectly conducting earth. It is observed that the attenuation α is the same for both cases in a low frequency region. As the frequency increases, the attenuation when considering the earth-return admittance becomes greater than that in the conventional admittance case. At a certain frequency, the attenuation starts to decrease. The frequency is the same as the critical frequency f_c at which the value of N in (15), as well as the conductance G, become negative as explained in reference [22]. The attenuation does not reach zero, but takes a minimum value and then starts to increase in a higher frequency region when the internal impedance of a conductor is included as observed in Fig. 2.

From the above observation, it should be clear that the earth-return admittance due to an imperfectly conducting earth affects the attenuation on a conductor. If the earth is assumed as perfectly conducting for the admittance, as in most studies of wave propagation and transient characteristics on transmission lines and cables, the attenuation increases monotonously as frequency increases. When a real earth which is imperfectly conducting is considered, the attenuation starts to decrease at the critical frequency f_c. This frequency region is called "Sommerfeld-Goubau propagation region" by Kikuchi, where transition occurs between TEM mode propagation (earth-return wave) and TM mode propagation [11, 15], or it is said that displacement currents become dominant over conduction currents in air.

IV. Numerical Electromagnetic Analysis

A. NEC Simulation

NEC is a numerical electromagnetic analysis method based on the Method of Moment (MoM) in frequency domain developed in the Lawrence Livermore National Laboratory [23]. Because a conductor is represented by a combination of cylindrical cells, the NEC can easily deal with the conductor with an arbitrary cross-section and also with a thin wire, which is not so easy when using Finite-Differences Time-Domain (FDTD) method [24]. In this section, the transition between propagation modes is investigated based on NEC simulations [26].

A1. Model Circuit

The overhead conductor with length x_0 and radius r is placed at a height h from the earth surface. The conductor resistivity ρ_c is 1×10^{-8} [Ω-m]. A sinusoidal voltage source $v_0(t) = V_0 \sin(\omega t)$ is applied to the conductor. The terminating resistance Z_r is taken as 469Ω for a matching condition.

The conductor length is taken to be $x_0 = 3000$ m or 1000 m depending on the frequency of the source voltage due to the limit of CPU memory required for a simulation with NEC. Table 1 shows an example of the number of conductor segments used to represent a conductor in NEC, because the segment length needs to be smaller when the frequency becomes higher, i.e. when the wave length becomes smaller.

TABLE 1 THE NUMBER OF SEGMENTS TO REPRESENT A CONDUCTOR IN NEC

Frequency [MHz]	10	20	50	60	100
Distance [m]	3000	3000	3000	1000	1000
Number of Segments	6000	8000	12000	5000	8000

A2. Simulation Results

A2.1 Amplitude Characteristic of Current along Conductor

Fig. 3 shows the current amplitude I_x at a distance x from the sending end for $h = 1$ m and $\varepsilon_r = 20$. The current waveform is given theoretically in the following form [28].

$$i_x(t) = I_0 \exp(-\alpha x) \cdot \sin(\omega t - \beta x) = I_x \sin(\omega t - \beta x) \qquad (17)$$

where $I_x = I_0 \exp(-\alpha x)$ is the current amplitude ($I_0 = I_x$ for $x = 0$), $\omega = 2\pi f$ is the voltage source frequency, α is the attenuation constant, and β is the phase constant.

Fig. 3(a) is for the frequency range from 10 MHz to 50 MHz, and Fig. 3(b) for 60 MHz to 100 MHz. It is observed in Fig. 3(b) that the current amplitude is inversely proportional to the distance x, and it is logarithmically linear. That is:

$$\ln(I_x) \propto -x$$

The above equation agrees with the theoretical formula in (17) neglecting the phase angle, i.e.

$$I_x = I_0 \exp(-\alpha x) \qquad (18)$$

In Fig. 3(a), however, the amplitude I_x is not logarithmically linear, but there exists an inflection point at around $x = 750$ m. The characteristic of I_x can be expressed in the following form.

$$I_x = I_0 \exp(-\alpha_1 x) \text{ for } 0 \le x \le 700 \text{ m}$$
$$= I_0 \exp(-\alpha_2 x) \text{ for } 1000 \text{ m} \le \text{x} \le 3000 \text{ m}$$
$$\alpha_1 > \alpha_2 \qquad (19)$$

Such a phenomenon never occurs in TEM mode propagation and cannot be explained by a theory of TEM propagation. The phenomenon corresponds to the transition between TEM and TM/TE modes, as Kikuchi pointed out in his papers [11, 12], and it is called "Sommerfeld-Goubau" propagation [13-15]. In TE/TM mode wave propagation, it is possible to have different attenuation and phase angles along a conductor [29].

A2.2. Attenuation Constant

Figs. 2 and 4 show attenuation constant α as a function of frequency corresponding to Fig. 3. A real line in the figure is the attenuation constant evaluated by using Wise's earth-return admittance and the accurate earth-return impedance in (6), i.e. TL approach. The attenuation constant by the NEC is calculated from the current amplitude I_x shown in Fig. 3.

The same characteristic as that explained in Section III-A for Fig. 2 is observed in Fig. 4. In a frequency region higher than the critical frequency, wave propagation becomes "surface wave" [13-15], and thus the earth-return impedance has no impact, the conductor internal impedance becoming dominant. There exists a TM or TE mode of propagation in between the region where the earth-return impedance is dominant and the region where the conductor internal impedance becomes dominant.

It is noteworthy that the earth-return impedance formulas, such as Carson's and Pollaczek's ones, are not necessary in the high frequency region discussed above, because the earth-return has no impact on wave propagation.

In Figs. 2 and 4, it is observed that the NEC results are almost identical to those calculated by the TL approach (Wise's admittance and the accurate impedance in (6)) in a frequency region lower than the critical frequency. In a frequency region higher than the critical frequency, the attenuation constant given by NEC is different from that given by the TL approach, especially when the conductor height is small. The reason for this difference is partially caused by the finite length of the conductor [30] in the NEC simulation. It is not easy to take a conductor element smaller than that given in Table 1. The difference requires a further investigation in future.

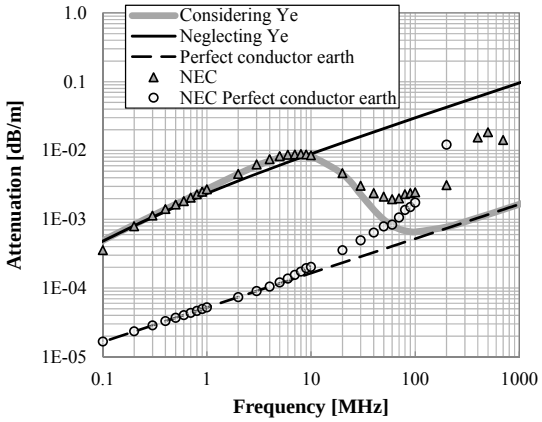

(a) $\varepsilon_r = 1$

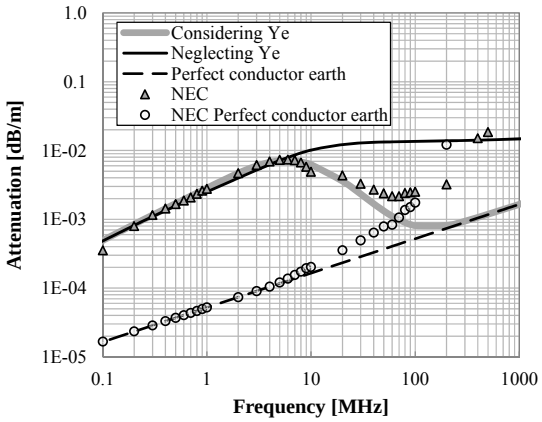

(b) $\varepsilon_r = 20$

Fig. 2. Frequency characteristics of attenuation considering the earth-return admittance: $h = 10$ m, $r = 1$ cm, $\rho_e = 100$ Ωm.

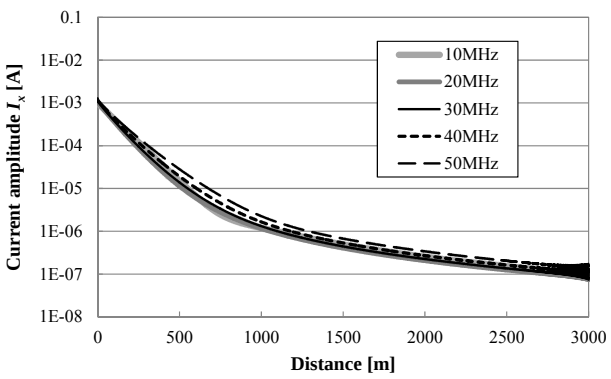

(a) $f = 10 – 50$MHz

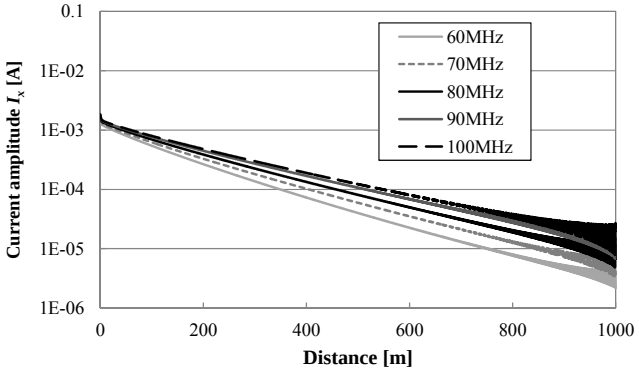

(b) $f = 60 – 100$MHz

Fig. 3. Amplitude characteristics along the conductor : h =1 m, r = 0.8 mm, ρ_e = 200 Ωm, ε_r = 20.

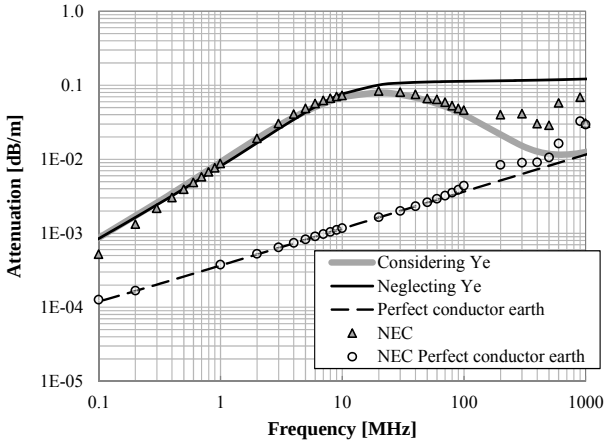

Fig. 4. Attenuation constant α as a function of frequency in comparison with that in Reference [22] : h =1 m, r = 0.8 mm, ρ_e = 200 Ω m, ε_r = 20.

A. FDTD Simulation

In this section, Sommerfeld-Goubau propagation is investigated based on FDTD (finite-difference time-domain) simulations [27]. Transient responses of electric and magnetic field strength along a conductor are calculated by the VSTL [25], based on the FDTD method, when a step-like voltage is applied to the sending end of the conductor. From the calculated results, wave propagation mode is estimated at the both ends and around the center of the conductor.

B.1. Model Circuit

Fig. 5 illustrates a model circuit for an FDTD simulation. A conductor with radius $r_1 = 1$ mm is covered by an insulator with radius $r_2 = 3$ mm and a relative permittivity ε_i. Table 2 gives the FDTD simulation conditions. The cell size is $\Delta s = 1$ mm. The absorbing boundary is adopted with instability-preventing coefficient $\alpha = 0.01$. The conductor height h is set to 6 cm. The conductor length x is 1 m and it is grounded through a matching resistance at the receiving end. A current waveform with a rise time of 10 ns is applied at the sending end. Table 3 summarizes the simulation results.

B2. Simulation results

B2.1. Comparison of lossy and perfectly conducting earth

Fig. 6 shows a comparison of transient responses of electric

field intensity E at the receiving end for y and z directions. The intensity for x direction is not shown because it is zero, which means the propagation mode is TEM.

No significant difference is observed between the perfectly conducting earth (Case 1) and the lossy earth (Case 3). This indicates that the wave propagation along the conductor is a so-called "surface wave" and thus the earth-return path has no contribution to the wave propagation, as already explained in the previous sections. The electric field intensity E_y in the y-direction decreases rapidly with y, i.e. when the separation from the conductor increases, as is well-known. A difference in E_y between Case 1 and Case 3 is observed in the time region from 10 ns to 20 ns, but no significant difference is observed after $t = 20$ ns. The difference comes from wave deformation due to the lossy earth, and the distortion dies out as time passes. This is also well-known in a transmission line theory [28].

Fig. 7 shows transient responses of magnetic field intensity H at the receiving end for y and z-directions (x-direction is not shown because $H_x = 0$). A similar trend to that of the electric field is observed for H between the perfectly conducting earth (Case 1) and the lossy earth (Case 3), although H_z is far greater than H_y whereas E_y is far greater than E_z.

TABLE 2. CONDITIONS FOR FDTD SIMULATIONS: $h = 6$ cm .

Case	Cable	Earth	
	ε_i	ρ [Ω.m]	ε_r
Case 1	1	0	1
Case 2	3	0	1
Case 3	1	100	1
Case 4	3	100	1
Case 5	1	100	10
Case 6	3	100	10
Case 7	1	2000	1
Case 8	3	2000	1

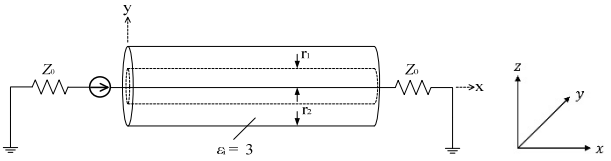

Fig. 5. A model circuit.

B2.2. Effect of outer insulation ε_i

Fig. 8 shows transient electric field strength E_x and E_y in the case of a lossy earth for a covered conductor. The electric field intensity E_z is not shown in the figure because E_z is similar to that in the case of a bare conductor shown in Fig. 6(b). E_x and E_y in the perfectly conducting earth case are similar to those in Fig. 6 except in the time region from $t = 10$ ns to 20 ns, as already explained in section B2.1.

In Fig. 8, it is observed that the wave propagation at the sending (not shown in Fig. 8) and receiving ends is a TM mode for E_x is not zero, while the wave propagation at the center ($x = 0.5$ m) is a TEM mode. The result agrees with the observation made by Goubau [14, 15], and clearly shows the transition between TM and TEM mode propagation. The transition is not observed in the bare conductor case as in Fig. 6, while it is observed in the TL approach and in the NEC simulation as in Figs. 2 and 5. The reason for this is estimated to be due to the very short conductor length (1 m). Fig. 2 is for an infinitely long conductor and Fig. 5 is for a length from 500 m to 3000 m. This requires a further investigation.

TABLE 3. FDTD SIMULATION RESULTS FOR WAVE PROPAGATION MODES.

x [cm]	y [mm]	Case 1, 3, 5, 7	Case 2, 4, 6	Case 8
0	3	TEM	TM	TM
	13		TEM	
	23			TEM
	53			
50	3	TEM	TEM	TEM
	13			
	23			
	53			
100	3	TEM	TM	TM
	13		TEM	
	23			TEM
	53			

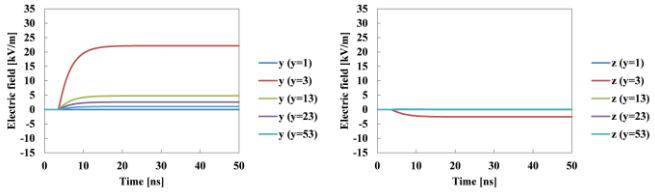

(a) Perfectly conducting earth: Case 1 (left: y direction; right: z direction).

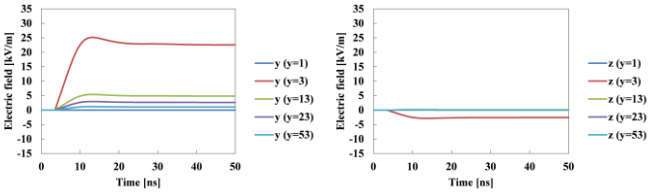

(b) Lossy earth: Case 3(left: y direction; right: z direction).

Fig. 6. Transient response of electric field intensity E on y-axis at $x = 1$ m.

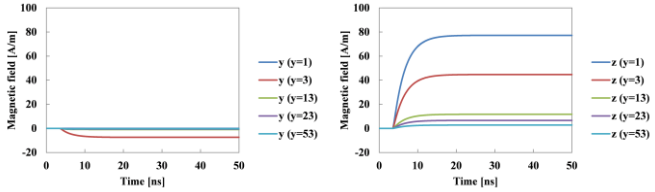

(a) Perfectly conducting earth: Case 1 (left: y direction; right: z direction).

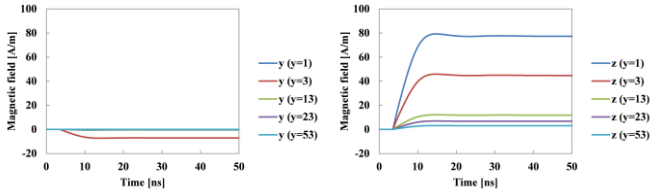

(b) Lossy earth: Case 3 (left: y direction; right: z direction).

Fig. 7. Transient response of magnetic field intensity H on y-axis at $x = 1$ m.

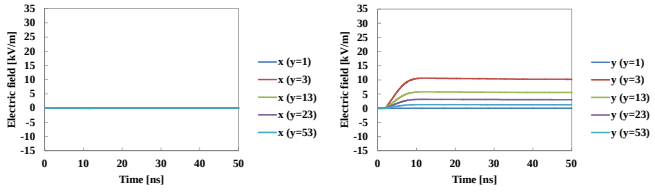

(a) $x = 0.5$ m (left: x direction; right: y direction).

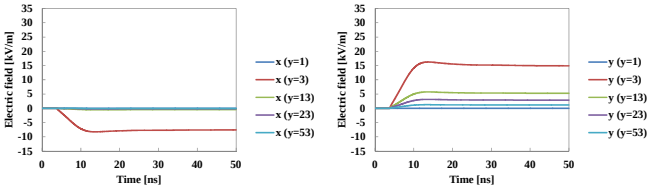

(b) x =1 m (left: x direction; right: y direction).

Fig. 8. Transient response of electric field intensity E for a covered conductor.

V. Conclusions

Well-known earth-return impedance formulas derived by Pollactek, Carson, and Sunde have been investigated, and it has been made clear that (1) Sunde's formula is not correct, (2) Pollactek's and Carson's formulas can deal with displacement currents as far as the relative earth permittivity is 1, (3) the stratified earth impedance is most general and Wise's correction of Carson's formula becomes identical to the formula for a homogeneous earth derived from the stratified one with $\mu_e = \mu_0$.

In a high frequency region where the surface wave is completed, the earth-return impedance has no contribution to the wave propagation, and thus it can be neglected.

Wave propagation in a high frequency region shows transition between TEM and TM modes. In a frequency lower than the critical frequency f_c, at which the transition called "Sommerfeld-Goubau propagation" starts, the wave propagation is determined by an earth-return path, which is called "earth-return wave propagation". In a frequency higher than the frequency of the transition region, so-called surface wave propagation, which is determined by the conductor internal impedance, is completed.

References

[1] F. Pollaczek, "Uber das feld einer unendlich langen wechselstrom durchlossenen einfachleitung," E.N.T., vol. 3, no. 9, pp. 339–359, 1926.

[2] J. R. Carson, "Wave propagation in overhead wires with ground return," Bell Syst. Tech. J., vol. 5, pp. 539–554, 1926.

[3] E. D. Sunde, "Earth conduction effects in transmission systems," Dover, New York, 1968.

[4] W. H. Wise, "Propagation of high-frequency currents in ground return circuits," Proc. I. R. E., vol. 22, no. 4, pp. 522–527, 1934.

[5] R. Rudenberg: "Transient performance of electric power system", MIT Press, 1969.

[6] D. K. Tran and J. Robert: "New study of parameters of EHV multi-conductor transmission lines with earth return", IEEE Trans. Power Apparatus and Systems, vol. 91, No. 2, pp. 452-458, 1972.

[7] C. Gary, "Approche complte de la propagation multifilaire en haute fréquence par l'utilization des matrices complexes," EDF Bulletin de la direction des études et recherches, Série B, no. 3/4, pp. 5-20, 1976.

[8] A. Deri, G. Tevan, A. Semlyen and A. Castanheira, "The complex ground return plane : a simplified model for homogeneous and multi-layer earth return," IEEE Trans. Power Apparatus and Systems, vol. 100, no. 8, pp. 3686–3693, 1981.

[9] F. Rachidi, C. A. Nucci, M. Ianoz and C. Mazzetti, "Influence of a lossy ground on lightning-induced voltages on overhead lines," IEEE Trans. on EMC, vol. 38, no. 3, pp. 250—264, 1996

[10] F. Rachidi, C. A. Nucci and M. Ianoz, "Transient analysis of multiconductor lines above a lossy ground," IEEE Trans. on Power Delivery, vol. 14, no. 1, pp. 294—302, 1999.

[11] H. Kikuchi, "Wave propagation on the ground return circuit in high frequency regions," J. IEE Japan, vol. 75 no. 805, pp. 1176–1187, 1955.

[12] H. Kikuchi, "Electro-magnetic field on infinite wire at high frequencies above plane-earth," J. IEE Japan, vol. 77, no. 825, pp. 721–733, 1957.

[13] A. Sommerfeld, "Fortpflanzung elektrodynamischer wellen an einem zylindrischen leiter," Ann. Phys. u. Chemie, vol. 67, pp. 233, Dec. 1899 (See J. A. Stratton, "Electromagnetic Theory," McGraw-Hill Book Co., New York, pp. 527, 1941).

[14] G. Goubau, "Surface wave and their application to transmission lines," J. A. Physics, vol. 21, issue 11, pp. 1119–1128, 1950.

[15] G. Goubau, "Single-conductor surface wave transmission lines," Proc. I. R. E, vol. 39, issue 6, pp. 619–624, 1951.

[16] M. Nakagawa, A. Ametani and K. Iwamoto, "Further studies on wave propagation in overhead lines with earth return: impedance of stratified earth," Proc. IEE, vol. 120, no. 12, pp. 1521–1528, 1973.

[17] A. Ametani, "Stratified earth effects on wave propagation – frequency-dependent parameters –," IEEE Trans. Power Apparatus and Systems, vol. 93, no. 5, pp. 1233–1239, 1974.

[18] A. Ametani, Y. Miyamoto and J. Mahseredjian , "Derivation of earth-return impedance of an overhead multi-conductor considering displacement currents", IEEJ Trans. Power & Energy, vol.B-134, no.11, pp.936-940 , Nov. 2014

[19] W. H. Wise, "Potential coefficients for ground return circuits," Bell Syst. Tech. J., vol. 27, pp. 365–371, 1948.

[20] M. Nakagawa, "Admittance correction effects of a single overhead line," IEEE Trans. Power Apparatus and Systems, vol. 100, no. 3, pp. 1154–1161, 1981.

[21] M. Nakagawa, "Further studies on wave propagation along overhead transmission lines: Effects of admittance correction," IEEE Trans. Power Apparatus and Systems, vol. 100, no. 7, pp. 3626–3633, 1981.

[22] A. Ametani, Y. Miyamoto, Y. Baba, and N. Nagaoka: "Wave propagation on an overhead multiconductor in a high frequency region", IEEE Trans. EMC, vol. 56, no. 6, pp. 1638-1648, 2014.

[23] G. J. Burke, A. J. Poggio, "Numerical electromagnetic code (NEC) – Method of Moments", Technical Document 116, Naval Ocean Systems Center, San Diego, 1980.

[24] CIGRE WG C4.501, "Guideline for numerical electromagnetic analysis method and its application to surge phenomena", CIGRE TB-543, 2013.

[25] http://criepi.denken.or.jp/jp/electric/facilitySoft/software_02.html

[26] Y. Miyamoto, A. Ametani, Y. Baba and N. Nagaoka: "Study on the attenuation of high frequency surge propagating along a horizontal conductor above lossy ground using the method of moment", IWHV 2014, Paper HV-14-107, Okinawa, Japan, Nov. 2014.

[27] T. Asada, Y. Miyamoto, A. Ametani, N. Nagaoka and Y. Baba, "An investigation of wave propagation modes on a conductor in high frequencies', Science & Engineering Review, Doshisha University, vol. 55, no.3, pp.225-235, 2014

[28] A. Ametani, "Distributed-Parameter Circuit Theory," Corona Publishing Co., Tokyo, 1990.

[29] K. Tanabe, T. Kawamoto and A. Tatematsu: "Propagation characteristics of EM waves in UHF band on conductors and its application to criteria distinguished real and false noise sources", CRIEPI Research Report H08015, September 2009 (in Japanese).

[30] A. Ametani and T. Kawamura: "A method of lightning surge analysis recommended in Japan using EMTP", IEEE Trans. Power Delivery, vol. 20, no. 2, pp. 867-875, April 2005.